Virial coefficients for trapped Bose and Fermi gases beyond the unitary limit: An *S*-matrix approach

Edgar Marcelino,[1] André Nicolai,[2] Itzhak Roditi,[2] and André LeClair[3]
[1]*Institut für Theoretische Physik III, Ruhr-Universität Bochum, Universitätsstraße 150, DE-44801 Bochum, Germany*
[2]*Centro Brasileiro de Pesquisas Físicas, Rua Dr. Xavier Sigaud 150, 22290-180 Rio de Janeiro, Rio de Janeiro, Brazil*
[3]*Department of Physics, Cornell University, 14850 Ithaca, New York, USA*
(Received 15 July 2014; published 17 November 2014)

We study the virial expansion for three-dimensional Bose and Fermi gases at finite temperature using an approximation that only considers two-body processes and is valid for high temperatures and low densities. The first virial coefficients are computed and the second is exact. The results are obtained for the full range of values of the scattering length, and the unitary limit is recovered as a particular case. A weak coupling expansion is performed and the free case is also obtained as a proper limit. The influence of an anisotropic harmonic trap is considered using the local density approximation (LDA), analytical results are obtained, and the special case of the isotropic trap is discussed in detail.

DOI: 10.1103/PhysRevA.90.053619 PACS number(s): 03.75.Hh, 03.75.Mn, 05.45.Mt

I. INTRODUCTION

The advances in experimental results and simulations on cold atoms [1–12] requires new methods for theorists to study these systems and explore similar ones. Analytical methods continue to be a powerful tool to explore these systems, although they generally provide approximate results, in comparison with numerical methods [13].

This work uses a formalism for statistical mechanics based on the S matrix [14]. It provides an expression of the free energy at finite temperature and density built on an integral equation of the pseudoenergy with a kernel based on the logarithm of the two-body S matrix at zero temperature. This integral equation is quite similar to the Yang-Yang equations used in the thermodynamical Bethe ansatz (TBA) [15].

The method is a "foam diagram" approximation which is valid for high temperatures and low densities and considers only contributions from two-body processes to the free energy. It is explained in [16] and has been already used to study the thermodynamical and critical properties of quantum gases in two and three dimensions in the unitary limit [17,18] and beyond the unitary limit in three dimensions [19]. In [20] the method was used to calculate the ratio of the viscosity to entropy density and the results were in good agreement with experimental data [21].

In [19] it was shown how this method may be used to obtain the coefficients of the virial expansion for quantum gases and the first four virial coefficients were calculated in three dimensions in the unitary limit. The second coefficient provided by this method is exact and agrees with the result in [22]. The third one in the unitary limit does not agree with the exact value obtained in [23,24] where three-body processes were considered, since the three-body processes are neglected in our approximation. The present work extends this analysis to arbitrary scattering length; the unitary limit is obtained as the scattering length goes to infinity. These remarks apply to both bosons and fermions, and both cases are considered here, whereas the literature mainly deals with fermions in the unitary limit.

Since Feshbach Resonance experiments allow us to adjust the scattering length to any finite value, there is no reason to study only the unitary limit, in which the scattering length diverges. Here we calculate the first three virial coefficients for both Bose and Fermi gases in three dimensions for different values of the dimensionless ratio

$$\alpha = \frac{\lambda_T}{a},$$

where $\lambda_T = \sqrt{\frac{2\pi}{mT}}$ is the de Broglie thermal wave length and a is the scattering length. The unitary limit results obtained in [19] are recovered in the proper limit and also the free case where the scattering length is tuned to zero. For large positive scattering length, molecules are formed and this is not considered in this work. However, in the "upper branch" [25–31] there are no molecules and our formalism may be applied. This situation is studied here because we consider the possibility that a Bose gas may stay in a metastable state before undergoing mechanical collapse [32]. Virial coefficients on the upper branch have not been considered before, to our knowledge.

Analytical expressions are obtained for a weak coupling expansion and they are compared to the previous results. The second virial coefficient is the only exact one (besides the first one) for the same reasons as in [19], and this will be discussed here. Finally the influence of a harmonic trap on the virial coefficients will be studied using the local density approximation (LDA), and analytic results will be obtained for the case of an anisotropic harmonic trap. The particular case of the isotropic trap will be discussed and some plots will be shown.

In the next section we present a brief summary of the formalism (for more details see [16]), the actions of our physical systems, and the conventions used in this paper. In Sec. III we derive the expression of the virial coefficients in terms of the two-body kernel of the theory in the foam diagram approximation in a different way than in [19]. In Sec. IV we obtain the first four virial coefficients of a Bose and a Fermi gas in three dimensions in terms of the ratio $\alpha = \frac{\lambda_T}{a}$ and discuss these results. In Sec. V we perform a weak coupling expansion and obtain analytical expressions for the virial coefficients in this situation, then we compare these results with the previous ones obtained in Sec. IV. In Sec. VI we study the influence of a trap on the virial coefficients using the local density approximation.

II. FORMALISM AND CONVENTIONS

In this section we review the main result in [16]. The formalism is developed starting with the fundamental formula [14] for the partition function Z:

$$Z = Z_0 + \frac{1}{2\pi}\int dE\, e^{-\beta E}\,\mathrm{Tr}\,\mathrm{Im}\partial_E \ln \hat{S}(E), \tag{1}$$

where Z_0 is the partition function for the free theory, $\beta = 1/T$ is the inverse temperature, and $\hat{S}$ is the S-matrix operator in scattering theory. A considerable amount of work is needed to turn this into a useful expression, such as the cluster expansion for the S matrix. The result is a diagrammatic expansion for the free energy, not to be confused with finite temperature Feynman diagrams which are perturbative in the coupling. Rather, diagrams consist of vertices with $2n$ legs which correspond to the logarithm of the n-particle to n-particle S matrix at zero temperature, up to some kinematical factors. (For nonrelativistic theories there is no particle production.) These vertices are connected by lines which are the occupation numbers

$$f_0(\mathbf{k}) = \frac{z}{e^{\beta\omega_{\mathbf{k}}} - s\,z}, \tag{2}$$

where s is a statistical parameter (1 for bosons and -1 for fermions) and $z = e^{\beta\mu}$ is the fugacity, where μ is the chemical potential. Here we are only considering non-relativistic theories where $\omega_{\mathbf{k}} = \mathbf{k}^2/2m$, m being the mass of the particles.

For the nonrelativistic theories we will consider, the two body S matrix, i.e., $n = 2$, can be calculated exactly, i.e., to all orders in the coupling, thus this formalism captures some nonperturbative aspects. However the vertices for $n > 2$ are difficult to calculate. Thus we consider the approximation where we consider only diagrams involving two-body scattering. These are the diagrams shown in Fig. 1, i.e., the "foam" diagrams. This infinite class of diagrams can be summed up, leading to an integral equation we describe below.

In this formalism, the filling fractions, or occupation numbers, are parametrized in terms of a pseudoenergy $\varepsilon(\mathbf{k})$ which has the same form as the free theory, i.e., the density has the following expression:

$$n = \int \frac{d^3\mathbf{k}}{(2\pi)^3}\frac{1}{e^{\beta\varepsilon(\mathbf{k})} - s}, \tag{3}$$

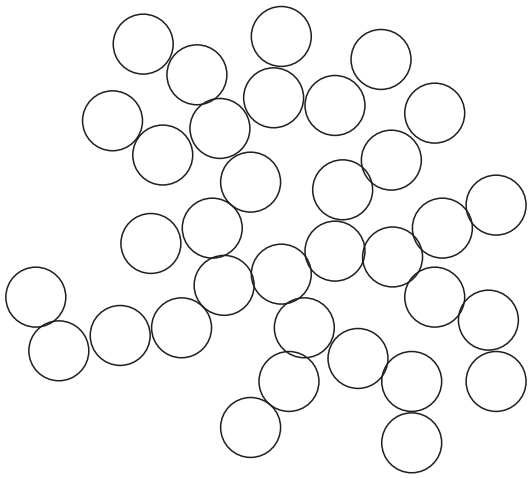

FIG. 1. Foam diagrams.

The summation of all foam diagrams leads to an integral equation satisfied by ε which we now describe. It is convenient to define

$$y(\mathbf{k}) = e^{-\beta\varepsilon(\mathbf{k}) - \omega_{\mathbf{k}} + \mu)}. \tag{4}$$

It satisfies the integral equation

$$y(\mathbf{k}) = 1 + \beta\int \frac{d^3\mathbf{k}'}{(2\pi)^3}\, G(\mathbf{k}-\mathbf{k}')\frac{z}{e^{\beta\omega_{\mathbf{k}'}} - s\,z\,y(\mathbf{k}')}. \tag{5}$$

The kernel G is the logarithm of the two-body S matrix multiplied by a kinematical factor which will be specified below. The pseudoenergy ε may be interpreted as a self-energy correction in the presence of all the particles of the gas that takes into account multiple scatterings, however our formalism is different than others in the literature that can also be interpreted as self-energies. It is different than the "self-consistent T-matrix approximation" for instance, since the latter does not involve our kernel G. The free energy is given by the following formula:

$$F = -\frac{1}{\beta}\int \frac{d^3\mathbf{k}}{(2\pi)^3}\left[-s\ln(1 - se^{-\beta\varepsilon(\mathbf{k})}) - \frac{1}{2}\left(\frac{1 - y(\mathbf{k})^{-1}}{e^{\beta\varepsilon(\mathbf{k})} - s}\right)\right]. \tag{6}$$

We will study both Bose and Fermi gases. The Bose gas will be described by the action

$$S = \int d^3\mathbf{x}\,dt\left(i\phi^\dagger\partial_t\phi - \frac{\nabla\phi^2}{2m} - \frac{g}{2}(\phi^\dagger\phi)^2\right) \tag{7}$$

and the fermion gas by

$$S = \int d^3\mathbf{x}\,dt\left(\sum_{\alpha=\uparrow,\downarrow} i\psi_\alpha^\dagger\partial_t\psi_\alpha - \frac{\nabla{\psi_\alpha}^2}{2m} - g\psi_\uparrow^\dagger\psi_\uparrow\psi_\downarrow^\dagger\psi_\downarrow\right). \tag{8}$$

The renormalized coupling constant is given by

$$\frac{1}{g_R} = \frac{1}{g} + \frac{m\Lambda}{2\pi^2}, \tag{9}$$

where Λ is the momentum cutoff introduced to regularize loop integrals. The scattering length is related to the renormalized coupling constant by

$$a = \frac{mg_R}{4\pi}. \tag{10}$$

In the unitary limit, the scattering length $a \to \pm\infty$ and the theory is scale invariant, i.e., at the renormalization group fixed point.

The two-body S matrix is

$$S_{\mathrm{matrix}}(|\mathbf{k}-\mathbf{k}'|) = \frac{8\pi/mg_R - i|\mathbf{k}-\mathbf{k}'|}{8\pi/mg_R + i|\mathbf{k}-\mathbf{k}'|} \tag{11}$$

and in the unitary limit it simply equals -1. The kernel that follows from this S matrix is

$$G(\mathbf{k},\mathbf{k}') = -\frac{16\pi\sigma}{m|\mathbf{k}-\mathbf{k}'|}\arctan\left(\frac{mg_R|\mathbf{k}-\mathbf{k}'|}{8\pi}\right), \tag{12}$$

where the factor σ that appears in (12) is $\sigma = 1/2$ for fermions and $\sigma = 1$ for bosons. Note that in the unitary limit the kernel remains a nonconstant but much simpler function, namely as $a \to \mp\infty$ one has

$$G(\mathbf{k}) = \pm\frac{8\pi^2\sigma}{m|\mathbf{k}|}. \tag{13}$$

In the present work, the first virial coefficients will be obtained for any value of the scattering length and the unitary limit will be recovered as $\alpha \to 0$.

III. EXPRESSIONS FOR THE VIRIAL COEFFICIENTS IN THE FOAM DIAGRAM APPROXIMATION

The virial coefficients b_i may be defined by the following expression:

$$F = -\frac{1}{\beta\lambda_T^3}\sum_{n=1}^{\infty} b_n z^n. \tag{14}$$

It is convenient to define a dimensionless scaling function q for the density of particles which is only a function of μ/T and $\alpha = \lambda_T/a$, as follows:

$$q = n\lambda_T^3. \tag{15}$$

Recalling that $n = -\frac{\partial F}{\partial \mu}$ one obtains

$$q = \sum_{n=1}^{\infty} n\, b_n z^n. \tag{16}$$

Substituting (3) in (15) and using (4), it is possible to expand q as follows:

$$q = \left(\frac{1}{2\pi mT}\right)^{3/2}\int d^3\mathbf{k}\, z\, y(\mathbf{k}) \times e^{-\beta\omega_{\mathbf{k}}}[1 + szy(\mathbf{k})e^{-\beta\omega_{\mathbf{k}}} + z^2y^2(\mathbf{k})e^{-2\beta\omega_{\mathbf{k}}} + \cdots]. \tag{17}$$

Using (4) and (5) it is possible to expand $y(\mathbf{k})$:

$$y(\mathbf{k}) = 1 + \frac{\beta}{(2\pi)^3}\int d^3\mathbf{k}' G(\mathbf{k},\mathbf{k}')\, z \times e^{-\beta\omega_{\mathbf{k}'}}[1 + s\, z\, y(\mathbf{k}')\, e^{-\beta\omega_{\mathbf{k}'}} + z^2y^2e^{-\beta\omega_{\mathbf{k}'}} + \cdots]. \tag{18}$$

Now, using (17) and (18) we can express the scaling function q in terms of the fugacity. Comparing to (16) one can then obtain expressions for the virial coefficients. The first three are

$$(2\pi mT)^{3/2}\, b_1 = \int d^3\mathbf{k}\, e^{-\beta\omega_{\mathbf{k}}}, \tag{19}$$

$$2(2\pi mT)^{3/2}\, b_2 = s\int d^3\mathbf{k}\, e^{-2\beta\omega_{\mathbf{k}}} + \frac{\beta}{(2\pi)^3}\int d^3\,\mathbf{k}d^3\mathbf{k}'\, e^{-\beta\omega_{\mathbf{k}}}e^{-\beta\omega_{\mathbf{k}'}}\, G(\mathbf{k},\mathbf{k}'), \tag{20}$$

$$3(2\pi mT)^{3/2}\, b_3 = \int d^3\mathbf{k}\, e^{-3\beta\omega_{\mathbf{k}}} + s\frac{2\beta}{(2\pi)^3}\int d^3\mathbf{k}\, d^3\mathbf{k}'\, e^{-2\beta\omega_{\mathbf{k}}}e^{-\beta\omega_{\mathbf{k}'}}\, G(\mathbf{k},\mathbf{k}') + \frac{\beta s}{(2\pi)^3}\int d^3\mathbf{k}\, d^3\mathbf{k}'\, e^{-\beta\omega_{\mathbf{k}}}e^{-2\beta\omega_{\mathbf{k}'}}\, G(\mathbf{k},\mathbf{k}'), \tag{21}$$

Evaluating the integrals that do not depend on the kernel, we obtain the simpler expressions

$$b_1 = 1, \tag{22}$$

$$2b_2 = \frac{s}{2^{3/2}} + \frac{\beta}{(2\pi)^3(2\pi mT)^{3/2}} \times \int d^3\mathbf{k}\, d^3\mathbf{k}'\, e^{-\beta\omega_{\mathbf{k}}}e^{-\beta\omega_{\mathbf{k}'}}\, G(\mathbf{k},\mathbf{k}'), \tag{23}$$

$$3b_3 = \frac{1}{3^{3/2}} + \frac{3\beta s}{(2\pi mT)^{3/2}(2\pi)^3} \times \int d^3\mathbf{k}\, d^3\mathbf{k}'\, e^{-2\beta\omega_{\mathbf{k}}}\, e^{-\beta\omega_{\mathbf{k}'}}\, G(\mathbf{k},\mathbf{k}'). \tag{24}$$

The above derivation of these expressions is slightly different than the one in [19], since it is not necessary to consider each diagram and find its contributions to the virial coefficients. The method presented in this paper automatically considers the foam diagram approximation because of the use of the integral equation (5); the fact that the results here are in agreement with [19] shows the consistency of the formalism presented in [16].

The second virial coefficient is exact, as was shown previously in the unitary limit [19]. Higher coefficients have contributions from two-body scattering, but since we do not take into account primitive higher body processes they give less precise results. For completeness, we give the contribution to b_4 from two-body interactions:

$$4b_4 = \frac{s}{4^{3/2}} + \frac{4\beta}{(2\pi mT)^{3/2}(2\pi)^3}\int e^{-3\beta\omega_{\mathbf{k}}}e^{-\beta\omega_{\mathbf{k}'}}\, G(\mathbf{k},\mathbf{k}')\, d^3\mathbf{k}\, d^3\mathbf{k}' + \frac{2\beta}{(2\pi)^3(2\pi mT)^{3/2}}\int e^{-2\beta\omega_{\mathbf{k}}}e^{-2\beta\omega_{\mathbf{k}'}}\, G(\mathbf{k},\mathbf{k}')\, d^3\mathbf{k}\, d^3\mathbf{k}' + \frac{2\beta^2 s}{(2\pi mT)^{3/2}(2\pi)^6}\int e^{-\beta\omega_{\mathbf{k}}}e^{-2\beta\omega_{\mathbf{k}'}}e^{-\beta\omega_{\mathbf{k}''}}\, G(\mathbf{k},\mathbf{k}') \times G(\mathbf{k}',\mathbf{k}'')\, d^3\mathbf{k}\, d^3\mathbf{k}' d^3\mathbf{k}''. \tag{25}$$

IV. THE RESULTS FOR THE FIRST VIRIAL COEFFICIENTS

Substituting the kernel (12) in Eqs. (22), (23), (24) and performing the angular parts of the integrals, it is possible to write the first virial coefficients in terms of the ratio $\alpha = \lambda_T/a$.

The results are the following:

$$b_1 = 1 \tag{26}$$

$$b_2 = \frac{s\sqrt{2}}{8} - \frac{2\sqrt{2}\sigma}{\pi^2}\int_0^\infty v\, e^{-\frac{v^2}{2\pi}} \arctan\left(\frac{v}{\alpha}\right) dv, \tag{27}$$

$$b_3 = \frac{\sqrt{3}}{27} - \frac{16\sqrt{3}\sigma s}{9\pi^2}\int_0^\infty v\, e^{-\frac{2v^2}{3\pi}} \arctan\left(\frac{v}{\alpha}\right) dv. \tag{28}$$

For the sake of completeness we also give the expression of the fourth coefficient,

$$\begin{aligned} b_4 = {} & \frac{s}{32} - \frac{2\sigma}{\pi^2}\int_0^\infty v e^{-\frac{3v^2}{4\pi}} \arctan\left(\frac{v}{\alpha}\right) dv \\ & - \frac{\sigma}{\pi^2}\int_0^\infty v e^{-\frac{v^2}{\pi}} \arctan\left(\frac{v}{\alpha}\right) dv \\ & + \frac{128\sigma^2 s}{\pi^{5/2}}\int_0^\infty\int_0^\infty\int_0^\infty e^{-(u^2+v^2+4w^2)} \\ & \times \sinh(uw)\sinh(vw)\arctan\left(\frac{u\sqrt{\pi}}{\alpha}\right) \\ & \times \arctan\left(\frac{v\sqrt{\pi}}{\alpha}\right) uv\, du\, dv\, dw. \end{aligned} \tag{29}$$

In the unitary limit, the above integrals can be evaluated analytically [19]. For a finite scattering length a, the integrals can only be done numerically.

The second virial coefficient as a function of α is plotted in Fig. 2 for bosons and in Fig. 3 for fermions, Figs. 4 and 5 show the third virial coefficient for bosons and fermions respectively. The values of these coefficients in the free case and in the unitary limit are also indicated in these figures with dotted and dashed lines respectively, and one sees they are recovered in the proper limits $a \to 0$ and $a \to \infty$. Note that both b_2 and b_3 flip sign as one passes through the unitary limit and the scattering length changes from $+\infty$ to $-\infty$. This is due to the exclusion of the bound state for both b_2 and b_3 since our b_3 is still only based on two-body physics.

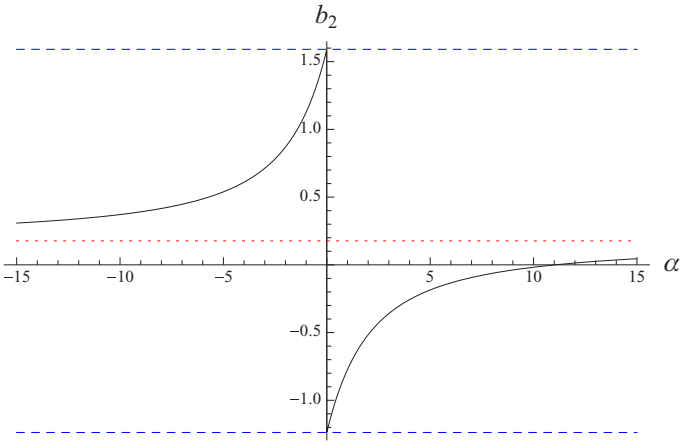

FIG. 2. (Color online) Second virial coefficient against the ratio between the thermal wavelength and the scattering length: $b_2 \times \alpha = \frac{\lambda_T}{a}$ for bosons (black). The values of the unitary limit ($\alpha \to 0^{\pm}$) obtained in [19] are represented by the dashed (blue) lines and the value of the free case ($g = 0 \Rightarrow \alpha \to \pm\infty$) is represented by the dotted (red) line.

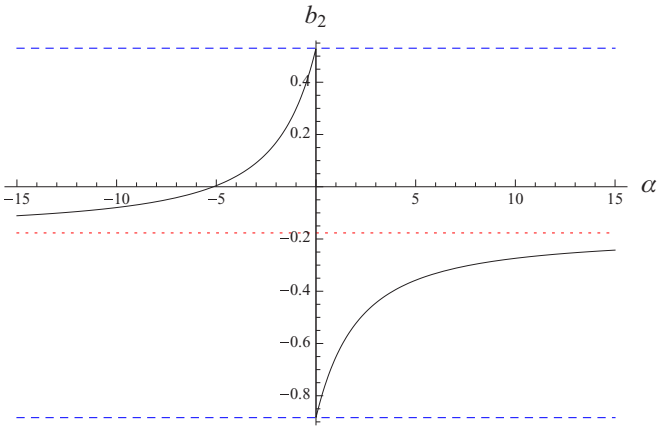

FIG. 3. (Color online) Second virial coefficient against the ratio between the thermal wavelength and the scattering length: $b_2 \times \alpha = \frac{\lambda_T}{a}$ for fermions (black). The values of the unitary limit ($\alpha \to 0^{\pm}$) obtained in [19] are represented by the dashed (blue) lines and the value of the free case ($g = 0 \Rightarrow \alpha \to \pm\infty$) is represented by the dotted (red) line.

Figures 2, 3, 4, and 5 show that the second and third virial coefficients are bounded by the values of the unitary limit case (when $\alpha \to 0$, the dashed lines) in the foam diagram approximation. When $g \to 0^{\pm} \Rightarrow \alpha \to \pm\infty$ (the dotted lines), the free case is always recovered as expected. The exact results for the values of the second coefficient in the unitary limit are also properly recovered for Bose and Fermi gases [19,22–24,33]. The expression (27) for fermions ($s = -1, \sigma = \frac{1}{2}$) is the same as the exact one obtained in [24], up to an integration by parts, thus our results for the second virial coefficient are exact for the whole range of α, as expected from our formalism.

The results in the unitary limit for the third coefficient obtained in [19] are recovered as expected. As discussed

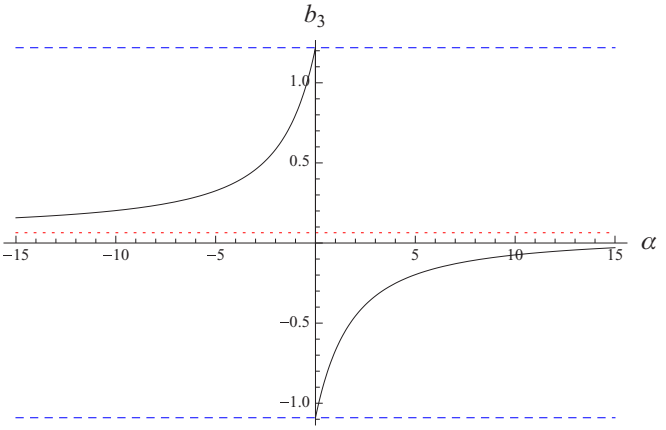

FIG. 4. (Color online) Third virial coefficient against the ratio between the thermal wavelength and the scattering length: $b_3 \times \alpha = \frac{\lambda_T}{a}$ for bosons (black). The values of the unitary limit ($\alpha \to 0^{\pm}$) obtained in [19] are represented by the dashed (blue) lines and the value of the free case ($g = 0 \Rightarrow \alpha \to \pm\infty$) is represented by the dotted (red) line.

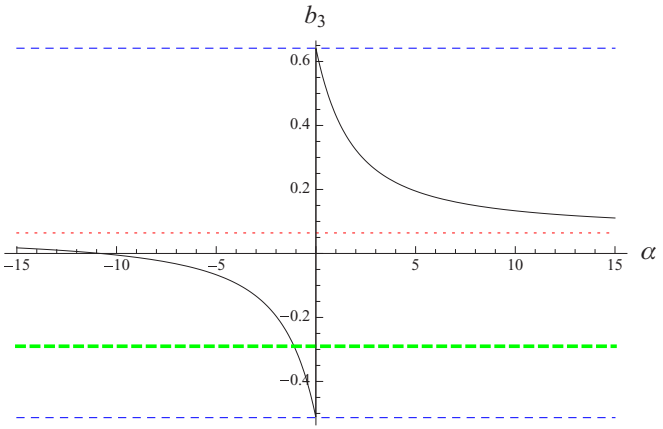

FIG. 5. (Color online) Third virial coefficient against the ratio between the thermal wavelength and the scattering length: $b_3 \times \alpha = \frac{\lambda_T}{a}$ for fermions (black). The values of the unitary limit ($\alpha \to 0^{\pm}$) obtained in [19] are represented by the dashed (blue) lines and the value of the free case ($g = 0 \Rightarrow \alpha \to \pm\infty$) is represented by the dotted (red) line. The exact result for the untarity limit with infinite negative scattering length obtained in [24] is represented by a thick dashed (green) line.

previously, they differ from the exact ones from [24,33,34] since the three-body processes are not considered in our approximation. As the ratio α increases, the interaction effects decrease and our results should become closer to the correct ones. Figure 5 indeed shows that for α sufficiently large the results obtained in [24] are nearly recovered; the exact value for this coefficient obtained in [24] for the unitary limit with large negative scattering length is also shown in this figure with a thick dashed line.

V. WEAK COUPLING EXPANSION

Expressions (27) and (28) give the virial coefficients in terms of the ratio $\alpha = \frac{\lambda_T}{a}$. In this section we perform an expansion for large values of α, which means that $\sqrt{T}\, g_R \ll 1$.

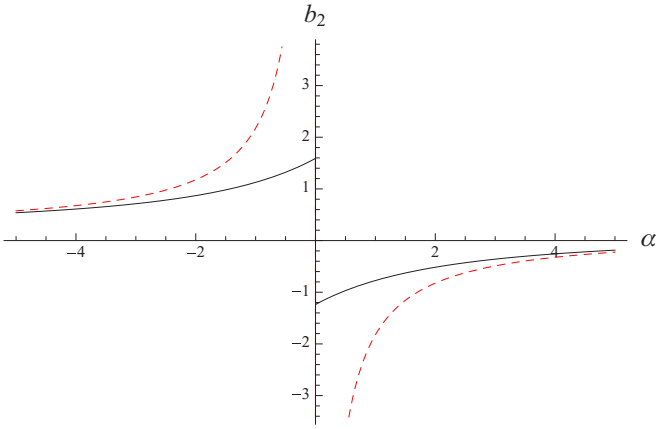

FIG. 6. (Color online) Second virial coefficient against the ratio between the thermal wavelength and the scattering length: $b_2 \times \alpha = \frac{\lambda_T}{a}$ for bosons (black). The dashed (red) line shows the same result obtained with the expression of the weak coupling expansion.

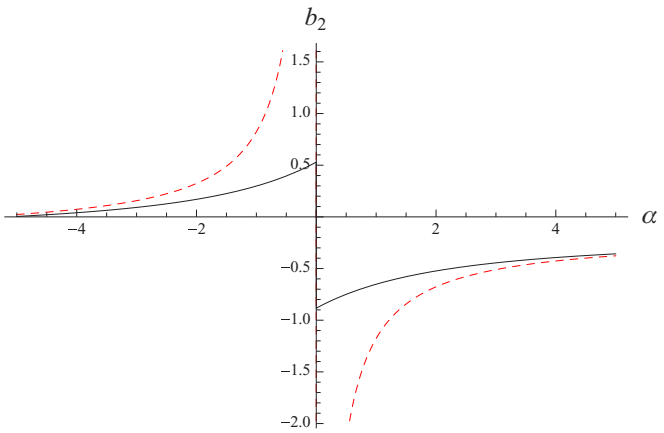

FIG. 7. (Color online) Second virial coefficient against the ratio between the thermal wavelength and the scattering length: $b_2 \times \alpha = \frac{\lambda_T}{a}$ for fermions (black). The dashed (red) line shows the same result obtained with the expression of the weak coupling expansion.

Since the temperature cannot be too small because we are under the foam diagram approximation, the coupling constant g_R should be very small in order for this expansion be valid.

One can simply expand the arctangent function in expressions (27) and (28) in a Taylor series, truncate it to the first degree term of $\frac{1}{\alpha}$, and evaluate the integrals analytically. Performing this expansion, one obtains

$$b_2 = \frac{s\sqrt{2}}{8} - \frac{2\sigma}{\alpha} \tag{30}$$

and

$$b_3 = \frac{\sqrt{3}}{27} - \frac{\sqrt{2}\sigma s}{\alpha}. \tag{31}$$

Figure 6 shows the second virial coefficient for bosons against α in the weak coupling approximation and the numerical result obtained in the latest section; Fig. 7 does the same for the fermionic situation and Figs. 8 and 9 do the same for the third coefficient of bosons and fermions respectively.

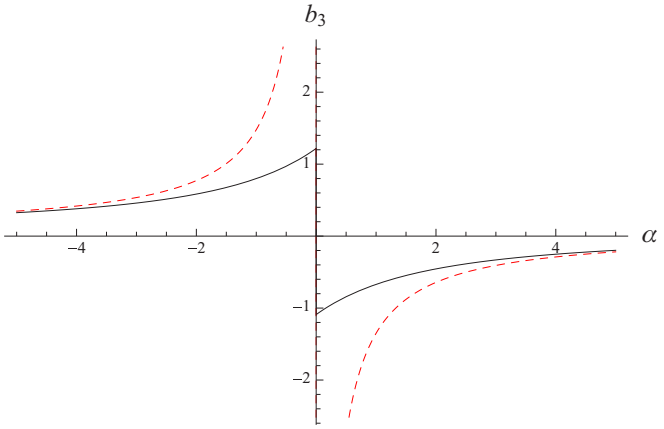

FIG. 8. (Color online) Third virial coefficient against the ratio between the thermal wavelength and the scattering length: $b_2 \times \alpha = \frac{\lambda_T}{a}$ for bosons (black). The dashed (red) line shows the same result obtained with the expression of the weak coupling expansion.

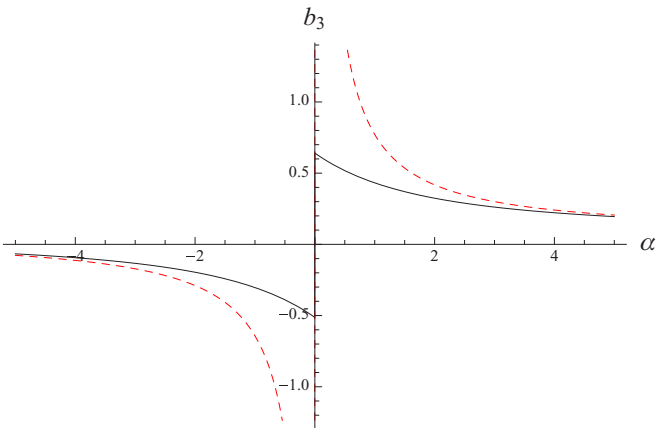

FIG. 9. (Color online) Third virial coefficient against the ratio between the thermal wavelength and the scattering length: $b_2 \times \alpha = \frac{\lambda_T}{a}$ for fermions (black). The dashed (red) line shows the same result obtained with the expression of the weak coupling expansion.

It is easy to see that the curves corresponding to Eqs. (30) and (31) and the ones obtained numerically integrating the expressions (27) and (28), shown in Figs 6, 7, 8, and 9, are almost indistinguishable for $|\alpha| > 4$.

VI. VIRIAL COEFFICIENTS FOR TRAPPED GASES

In order to study the influence of a harmonic trap for quantum gases it is possible to use the local density approximation (LDA). The LDA may be used if one ignores the variation of thermodynamic quantities due to density gradients [35,36]. In our formalism this means that one can replace the chemical potential by $\mu \to \mu - V(\mathbf{r})$, giving a free energy $F(\mathbf{r})$ that depends on $\mathbf{r}$. The final free energy will be given by $F = \int F(\mathbf{r}) d^3\mathbf{r}$.

We know that the virial cofficients are related to the free energy by Eq. (16). Therefore, in the LDA approximation, expression (16) becomes

$$F = -\frac{1}{\beta\lambda^3}\sum_{n=1}^{\infty}\left(b_n \int e^{-\beta n V(\mathbf{r})} d^3\mathbf{r}\right) z^n. \tag{32}$$

Comparing (32) to (16) one sees that the presence of the trap changes the virial coefficients in the following way under the LDA approximation:

$$b_n \to b_n \int e^{-\beta n V(\mathbf{r})} d^3\mathbf{r}. \tag{33}$$

Considering an anisotropic harmonic trap

$$V(\mathbf{r}) = \sum_{i=1}^{3}\left[\frac{w_i x_i^2}{2}\right]$$

we obtain

$$b_n \to b_n \left(\frac{2\pi}{\beta n}\right)^{\frac{3}{2}} \left[\prod_{i=1}^{3} w_i\right]^{-\frac{1}{2}}. \tag{34}$$

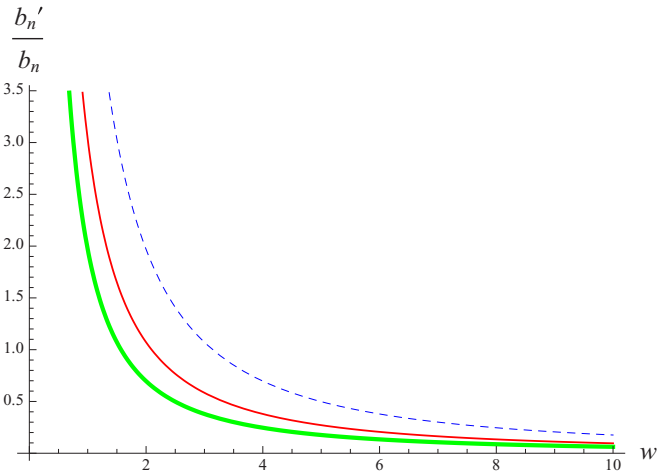

FIG. 10. (Color online) Ratio between the second, third, and fourth virial coefficients in the presence and in the absence of an harmonic isotropic trap against the frequency of the trap for $T = 1$ in the three-dimensional case ($d = 3$), $\frac{b_n'}{b_n} \times w$. $n = 2$ is the dashed (blue) line, $n = 3$ is the thin (red) line, and $n = 4$ is the thick (green) line.

In particular, if the trap is isotropic, $w_1 = w_2 = w_3 = w$, we arrive at the following result:

$$b_n \to b_n \left(\frac{2\pi}{\beta w n}\right)^{\frac{3}{2}}. \tag{35}$$

One sees that for w given by the fundamental Matsubara frequency $\frac{2\pi}{\beta}$, the first virial coefficient b_1 does not change in the presence of the harmonic isotropic trap. In the following figures we plot the ratios b_n'/b_n for $n = 2,3,4$, where $'$ means the presence of the harmonic isotropic trap, as a function of w for $T = 1$, and also as a function of T for $w = 1$.

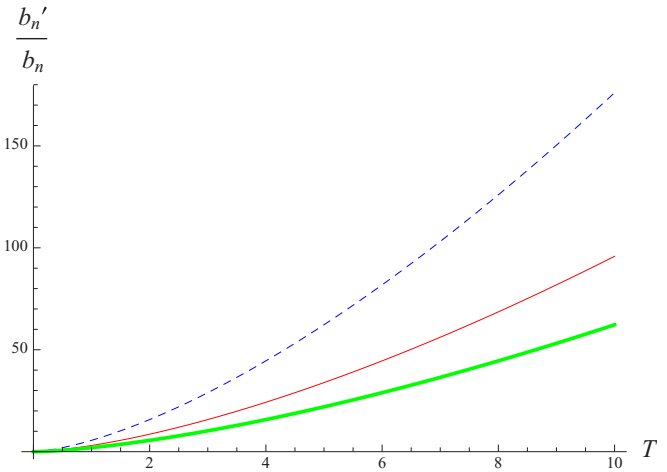

FIG. 11. (Color online) Ratio between the second, third, and fourth virial coefficients in the presence and in the absence of an harmonic isotropic trap against the temperature for $w = 1$ in the three-dimensional case ($d = 3$), $\frac{b_n'}{b_n} \times T$. $n = 2$ is the dashed (blue) line, $n = 3$ is the thin (red) line, and $n = 4$ is the thick (green) line.

Expressions (34) and (35) show that the virial coefficients decrease monotonically with the frequencies of the trap and increase monotonically with the temperature as a power law as Figs. 10 and 11 show for the isotropic case.

VII. CONCLUSIONS

The first virial coefficients of a bosonic and a fermionic gas were obtained as functions of the ratio of the thermal wavelength to the scattering length $\alpha = \frac{\lambda_T}{a}$ in the foam diagram approximation. The results obtained in [19] are recovered when $\alpha \to 0^{\pm}$ as expected and one also recovers the free case when $\alpha \to \pm\infty$.

The second virial coefficients are exact and the unitary limit values for the fermionic case agree with the results of [22] as is explained in [19]. The third coefficient is not exact since the foam diagram approximation neglects three-body interactions, however it becomes very close to the correct value when the absolute value of the ratio α is large.

A weak coupling expansion was performed and analytical expressions for the virial coefficients were obtained for large values of $|\alpha|$. The weak coupling expansion is in close agreement with the results we obtained for any α when $|\alpha| > 4$.

The influence of an anisotropic harmonic trap was also considered under the local density approximation and analytical expressions were obtained, and also specialized to an isotropic trap.

ACKNOWLEDGMENTS

The authors acknowledge financial support from CNPq, CAPES, and FAPERJ. This work is partly funded by a Science Without Borders CNPq grant.

[1] Y. Shin, C. Schunck, A. Schirotzek, and W. Ketterle, Nature (London) **451**, 689 (2008).
[2] I. Bloch, J. Dalibard, and W. Zwerger, Rev. Mod. Phys. **80**, 885 (2008).
[3] C. Chin, R. Grimm, P. Julienne, and E. Tiesinga, Rev. Mod. Phys. **82**, 1225 (2010).
[4] S. Nascimbène, N. Navon, K. J. Jiang, F. Chevy, and C. Salomon, Nature (London) **463**, 1057 (2010).
[5] K. Van Houcke, F. Werner, E. Kozik, N. Prokofev, B. Svistunov, M. J. H. Ku, A. T. Sommer, L. W. Cheuk, A. Schirotzek, and M. W. Zwierlein, Nat. Phys. **8**, 366 (2012).
[6] M. Horikoshi, S. Nakajima, M. Ueda, and T. Mukaiyama, Science **327**, 442 (2010).
[7] A. Minguzzi, S. Succi, F. Toschi, M. P. Tosi, and P. Vignolo, Phys. Rep. **395**, 223 (2004).
[8] E. Burovski, N. Prokof'ev, B. Svistunov, and M. Troyer, Phys. Rev. Lett. **96**, 160402 (2006).
[9] A. Bulgac, J. E. Drut, and P. Magierski, Phys. Rev. A **78**, 023625 (2008).
[10] P. Magierski, G. Wlazlowski, A. Bulgac, and J. E. Drut, Phys. Rev. Lett. **103**, 210403 (2009).
[11] Y. Castin and F. Werner, in *The BEC-BCS Crossover and the Unitary Fermi Gas*, Springer Lecture Notes in Physics Vol. 836, edited by W. Zwerger (Springer, Berlin, 2012), p. 127.
[12] H. Hu, X.-J. Liu, and P. D. Drummond, New J. Phys. **12**, 063038 (2010).
[13] J. R. Armstrong, N. T. Zinner, D. V. Fedorov, and A. S. Jensen, Phys. Rev. E **86**, 021115 (2012).
[14] R. Dashen, S.-K. Ma, and Herbert J. Bernstein, Phys. Rev. **187**, 1 (1969).
[15] C. N. Yang and C. P. Yang, J. Math. Phys. **10**, 1115 (1969).
[16] P. T. How and A. LeClair, Nucl. Phys. B **824**, 415 (2010).
[17] P.-T. How and A. LeClair, J. Stat. Mech. (2010) P03025.
[18] P.-T. How and A. LeClair, J. Stat. Mech. (2010) P07001.
[19] A. LeClair, E. Marcelino, A. Nicolai, and I. Roditi, Phys. Rev. A **86**, 023603 (2012).
[20] A. LeClair, New J. Phys. **13**, 055015 (2011).
[21] C. Cao, E. Elliot, J. Joseph, H. Wu, J. Petricka, T. Schäfer, and J. E. Thomas, Science **331**, 58 (2011).
[22] T. L. Ho and E. J. Mueller, Phys. Rev. Lett. **92**, 160404 (2004).
[23] X.-J. Liu, H. Hu, and P. D. Drummond, Phys. Rev. Lett. **102**, 160401 (2009).
[24] X. Leyronas, Phys. Rev. A **84**, 053633 (2011).
[25] K. Dieckmann, C. A. Stan, S. Gupta, Z. Hadzibabic, C. H. Schunck, and W. Ketterle, Phys. Rev. Lett. **89**, 203201 (2002).
[26] S. Jochim, M. Bartenstein, A. Altmeyer, G. Hendl, C. Chin, J. H. Denschlag, and R. Grimm, Phys. Rev. Lett. **91**, 240402 (2003).
[27] J. P. Gaebler, J. T. Stewart, T. E. Drake, D. S. Jin, A. Perali, P. Pieri, and G. C. Strinati, Nat. Phys. **6**, 569 (2010).
[28] S. Tsuchiya, R. Watanabe, and Y. Ohashi, Phys. Rev. A **80**, 033613 (2009).
[29] V. B. Shenoy and T.-L. Ho, Phys. Rev. Lett. **107**, 210401 (2011).
[30] F. Palestini, P. Pieri, and G. C. Strinati, Phys. Rev. Lett. **108**, 080401 (2012).
[31] W. Li and T.-L. Ho, Phys. Rev. Lett. **108**, 195301 (2012).
[32] W. Ketterle (private communication).
[33] D. B. Kaplan and S. Sun, Phys. Rev. Lett. **107**, 030601 (2011).
[34] Y. Castin and Félix Werner, Can. J. Phys. **91**, 382 (2013).
[35] F. Dalfovo and S. Giorgini, Rev. Mod. Phys. **71**, 463 (1999).
[36] F. Dalfovo and S. Stringari, Phys. Rev. A **53**, 2477 (1996).